In situ Visualization of therapeutic drug effects using phosphosite-specific GPCR antibodies

Sebastian Fritzwanker[1], Falko Nagel[2], Andrea Kliewer[1], Stefan Schulz[1,2,*]

[1] Institut für Pharmakologie und Toxikologie, Universitätsklinikum Jena, Friedrich-Schiller-Universität Jena, Drackendorfer Straße 1, D-07747 Jena, Germany

[2] 7TM Antibodies GmbH, Hans-Knöll-Straße 6, D-07745 Jena, Germany

[*]Corresponding author

Emails: stefan.schulz@med.uni-jena.de or stefan.schulz@7tmantibodies.com

Abstract

G protein-coupled receptors (GPCRs) are vital signal transducers that upon activation become phosphorylated on intracellular serine and threonine residues. Although antibodies that specifically recognize the phosphorylation state of GPCRs have been available for many years, efficient immunolocalization of phosphorylated receptors in their tissues of origin has remained elusive. Here we show that GPCR phosphorylation is very unstable during routine immunohistochemical procedures, necessitating the presence of appropriate phosphatase inhibitors throughout both fixation and staining procedures. We provide proof of concept using three out of four phosphorylation state-specific μ-opioid receptor antibodies and show that this approach can be readily extended to other prototypical GPCRs such as the CB1 cannabinoid receptor. In summary, this improved protocol will facilitate the widespread application of phosphorylation state-specific antibodies to monitor the physiological and pharmacological activation of endogenous GPCRs.

Introduction

Serine/threonine phosphorylation is the most important post-translational modification of GPCRs [1-5]. A widely used approach to analyze GPCR phosphorylation is the use of phosphosite-specific antibodies [6-9]. When available, such antibodies are valuable tools to elucidate the temporal dynamics of receptor phosphorylation, identify relevant kinases and phosphatases, and detect receptor activation using immunoblotting techniques[7, 10-15]. However, previous attempts using routine immunohistochemical approaches to unequivocally reveal agonist-induced phosphorylation of endogenous GPCRs in native tissues largely failed.

In intact cells, GPCR dephosphorylation is regulated in time and space, beginning immediately after receptor activation at the plasma membrane [16]. Indeed, phosphosite-specific antibodies in combination with siRNAs have led to the identification of distinct protein phosphatase 1 (PP1) and PP2 catalytic subunits as bona fide GPCR phosphatases [17-22]. For many receptors, dephosphorylation is complete within 10 to 30 minutes after agonist washout [17, 18, 21]. A notable exception is the agonist-induced phosphorylation of S341/S343 at the SST2 somatostatin receptor, which persists for considerably longer periods [21]. Consequently, activated SST2 receptors could be successfully localized using pS341/pS343-SST2 antibodies under routine immunohistochemical conditions [23]. However, this approach could not easily be reproduced for other SST2 sites or other GPCRs.

The ability to visualize activated and phosphorylated GPCRs in their tissues of origin would provide important clues to the physiological and pharmacological regulation of receptor activation. In particular, it would allow for distinction between currently-activated and resting GPCR populations in the context of particular physiological or behavioral conditions. We were therefore motivated to develop and validate immunohistochemical fixation and staining procedures that can be universally applied to prototypical GPCRs. Our

improved protocol will facilitate the widespread application of phosphosite-specific antibodies as biosensors for receptor activation in academic and pharmaceutical research.

Results

Dephosphorylation of GPCRs occurs rapidly in intact cells and is mediated by the protein phosphatases PP1 and PP2 [16]. Serine/threonine phosphatases are known to be activated during cell lysis and tissue fixation procedures. We therefore systematically tested the inclusion of appropriate protein phosphatase inhibitors (PPIs) during tissue fixation and/or immunohistochemical staining procedures. For this purpose, mice were treated with either methadone or saline, perfusion fixed, and slices of brain and spinal cord were stained with phosphosite-specific μ-opioid receptor (MOP) or phosphorylation-independent np-MOP antibodies. As expected, staining using the np-MOP antibody was present in the superficial layers of the spinal cord, regardless of drug treatment or the presence of phosphatase inhibitors (**Fig. 1**). In contrast, immunostaining for pT379-MOP was only detected in methadone-treated animals when a cocktail of appropriate phosphatase inhibitors was present during both tissue fixation and throughout the staining procedure (**Fig. 1**).

Four unique serine and threonine residues are phosphorylated in MOP in response to full agonists [8, 15]. Phosphosite-specific antibodies have been generated for all of these sites, which work equally well in immunoblot applications [7, 24, 25]. We found that three out of four, namely pS375-MOP, pT376-MOP and pT379-MOP, but not pT370-MOP, are also well suited for immunohistochemical staining of phosphorylated MOP under these conditions (**Fig. 2 upper panel**). Neither p-MOP nor np-MOP staining was apparent in MOP knockout mice (**Fig. 2 lower panel**).. To further substantiate the specific binding of phospho-MOP antibodies, we performed peptide neutralization controls. When pS375-MOP or pT379-MOP antibodies were incubated with an excess of their respective immunizing peptide containing

S375 or T379 in phosphorylated form, immunostaining was completely absent in the superficial layers of the spinal cord (**Fig. 3**). In contrast, immunostaining was virtually unaffected by the addition of the corresponding non-phosphorylated peptides, indicating unequivocal detection of agonist-dependent S375 and T379 phosphorylation of MOP (**Fig. 3**).

The antagonist naloxone drives MOP into an inactive state, preventing agonist-induced phosphorylation. When mice were treated with the selective MOP agonist fentanyl, we found the typical staining pattern for pS375-MOP, pT376-MOP and pT379-MOP as evidence of MOP activation. In contrast, this staining was not detected in animals injected with naloxone immediately prior to fentanyl challenge, indicating that MOP activation was blocked by the antagonist (**Fig. 4**). Next, we compared the immunostaining patterns obtained for phospho-MOP with total MOP obtained with an antibody that detects the receptor in a phosphorylation-independent manner. While there was good overlap in many brain regions, including habenula and fasciculus retroflex, neither pS375-MOP, pT376-MOP, nor pT379-MOP immunostaining was evident in the nucleus accumbens or caudate putamen (**Fig. 5**). These results suggest that region-specific MOP activation patterns exist, which can now be visualized for the first time.

The final set of experiments was designed to extend this new approach to another prototypical GPCR namely the CB1 cannabinoid receptor. In fact, the p425-CB1 antibody produced staining in hippocampus and cortex closely resembling that of the np-CB1 antibody only when mice were treated with CP-55940 but not in untreated mice [26] (**Fig. 6**). This staining was completely abolished when the p425-CB1 antibody was neutralized with its immunizing peptide or when CP-55940 action was blocked with antagonist (**Fig. 6**). At higher magnification it became apparent that in CP-55940- treated mice the p425-CB1 antibody exclusively labelled fibers and terminals similar to that seen with the np-CB1 antibody (**Fig. 7**).

Discussion

GPCRs are privileged targets for small molecule drugs in almost all therapeutic areas [27]. However, to date, the visualization of therapeutic drug effects on endogenously expressed GPCRs in native tissues has remained a major challenge. Activation of GPCRs by their endogenous ligands or exogenous agonists results in conformational changes that are recognized by a family of kinases termed G protein-coupled receptor kinases (GRKs) [1-5]. The unique ability of GRKs to recognize activated receptors results in agonist-dependent phosphorylation at intracellular serine and threonine residues [1-5]. Thus, analysis of agonist-driven phosphorylation of GPCRs can provide valuable insights into receptor activation. Antibodies that specifically recognize the GPCR phosphorylation state have been available in some cases over the last 20 years. Indeed, phosphosite-specific GPCR antibodies have proven useful to detect receptor activation and to profile the pharmacological properties of new ligands [12-15]. To date, however, their utility has been largely limited to immunoblotting approaches using heterologous receptor expression systems, while detection of phosphorylated GPCRs from tissue lysates has been mostly unsuccessful, due to their low abundance in vivo.

Here we have systematically developed an improved immunohistochemical staining procedure that allows for visualization of opioid drug effects in the mouse brain in vivo. We also show that this approach can be easily extended to other prototypical GPCRs such as the CB1 cannabinoid receptor. Key to this new protocol was the finding that GPCR phosphorylation is highly unstable during routine immunohistochemistry and that inclusion of protein phosphatase inhibitors was required during both the fixation and staining procedures. Several lines of evidence suggest that our approach facilitates the localization of bona fide phosphorylated GPCRs. First, phospho-GPCR immunostaining strongly increased when animals had been treated with agonist. Conversely, immunostaining was not detected when

agonist action was blocked by antagonist. Second, robust phospho-GPCR immunostaining was only apparent when appropriate protein phosphatase inhibitors were included in all steps of fixation and staining procedures. Third, phospho-GPCR immunostaining was completely neutralized by preincubation with cognate phosphorylated peptides but not with the corresponding non-phosphorylated peptides.

In summary, we provide a proof of concept for using phosphorylation state-specific antibodies as biosensors to elucidate GPCR activation in native tissues. Our approach not only facilitates the visualization of the effects of agonists and antagonists in preclinical animal studies, but also in human tissues. It also allows for elucidation of different cellular and subcellular activation patterns in response to external stimuli or drug administration. Therefore, phosphorylation state-specific antibodies are a new class of biomarkers of GPCR activation that are likely to find widespread application in academic and pharmaceutical research.

Figure legends

Fig. 1. Comparison of phospho-MOP immunohistochemistry in the presence or absence of protein phosphatase inhibitors. (A, B) Animals were either treated with methadone or saline for 30 min, transcardially perfused, fixed and stained in the presence (+) or absence (-) of protein phosphatase inhibitors (PPI). Shown are confocal images of coronal sections of the spinal cord stained with pT379-MOP or np-MOP antibody. Note that PPIs need to be present during both fixation and staining procedures to obtain agonist-induced phospho-MOP immunostaining. Scale bar = 250 µm.

Fig. 2. Immunohistochemical staining of agonist-induced MOP phosphorylation in the mouse spinal cord. Animals were treated with methadone or saline for 30 min, transcardially perfused, fixed and stained in the presence of PPIs. Shown are confocal images of coronal sections of the spinal cord stained with phosphosite-specific antibodies pT370-MOP, pS375-MOP, pT376-MOP and pT379-MOP, or phosphorylation independent np-MOP antibody. Note that pS375-MOP, pT376-MOP and pT379-MOP, but not pT370-MOP, revealed an agonist-dependent MOP phosphorylation immunostaining in a pattern closely resembling that of agonist-independent np-MOP imunostaining. Scale bar = 250 µm.

Fig. 3. Peptide neutralization of agonist-induced MOP phosphorylation staining in the mouse spinal cord. Animals were treated with methadone for 30 min, transcardially perfused, fixed and stained in the presence of PPIs. Shown are confocal images of coronal sections of the spinal cord stained with phosphosite-specific antibodies pS375-MOP or pT379-MOP in the presence or absence of their immunizing peptides containing S375 or T379 in phosphorylated form (p-Peptide) or the corresponding non-phosphorylated peptide (np-Peptide). Note that

phospho-MOP immunostaining was completely neutralized by excess of phosphorylated peptide but not of non-phosphorylated peptide. Scale bar = 250 µm.

Fig. 4. Antagonist block of phospho-MOP immunostaining. Animals were either treated with saline or fentanyl for 15 min. Where indicated, animals were pretreated with naloxone for 10 min followed by 15-min fentanyl treatment. Animals were then transcardially perfused, fixed and stained in the presence of PPIs. Shown are confocal images of coronal sections of the spinal cord stained with phosphosite-specific antibodies pS375-MOP, pT376-MOP or pT379-MOP or phosphorylation independent np-MOP antibody. Note that agonist-induced phospho-MOP immunostaining is diminished by antagonist treatment. Scale bar = 250 µm.

Fig. 5. Agonist-induced phospho-MOP immunostaining in mouse brain. Animals were treated with methadone for 30 min, transcardially perfused, fixed and stained in the presence of PPIs. Shown are confocal images of coronal brain sections stained with phosphosite-specific antibodies pS375-MOP, pT376-MOP or pT379-MOP or phosphorylation independent np-MOP antibody. Note that all three phosphosite-specific antibodies detected agonist-induced MOP phosphorylation in the medial habenula and fasciculus retroflexus but not in nucleus accumbens or caudate putamen, a brain regions known to be rich in MOP receptors as shown by np-MOP antibody staining. Scale bar = 250 µm.

Fig. 6. Agonist-induced phospho-CB1 immunostaining in mouse brain. Animals were either treated with Vehicle or CP-55940 for 30 min. Where indicated, animals were pretreated with AM251 for 45 min followed by 30-min CP-55940 treatment. Animals were then transcardially perfused, fixed and stained in the presence of PPIs. Shown are confocal images of coronal brain sections stained with phosphosite-specific antibody pS425-CB1, in the

presence or absence of the p-Peptide containing S425 in phosphorylated form, or phosphorylation independent np-CB1 antibody. Note that agonist-induced phopho-CB1 immunostaining is diminished by antagonist treatment. Note that phospho-CB1 immunostaining was completely neutralized by excess of phosphorylated peptide. Scale bar = 1000 µm and 250 µm.

Fig. 7. Agonist-induced phospho-CB1 immunostaining in mouse brain. Animals were either treated with Vehicle or CP-55940 for 30 min. Animals were then transcardially perfused, fixed and stained in the presence of PPIs. Shown are confocal images of coronal brain sections stained with phosphosite-specific antibody pS425-CB1. Note that agonist-induced phopho-CB1 immunostaining is localized to fibers and terminals in cortex and hippocampus. Scale bar = 100 µm.

Methods

Antibodies

The phosphorylation state-specific MOP antibodies pT370-MOP (7TM0319B), pS375-MOP (7TM0319C), pT376-MOP (7TM0319D), pT379-MOP (7TM0319E), pS245-CB1 antibody (7TM0056A) and the phosphorylation-independent antibodies np-MOP (7TM0319N) were provided by 7TM Antibodies (www.7tmantibodies.com). The np-MOP was from abcam (ab134054) and the np-CB1 antibody from Cayman (10006590).

Animals

Mice (JAXTM C57Bl/6J obtained from Charles River) were housed 2–5 per cage under a 12-hr light-dark cycle with ad libitum access to food and water. All animal experiments were approved by Thuringian state authorities and performed in accordance with European Commission regulations for the care and use of laboratory animals. Our study is reported in accordance with ARRIVE guidelines [28]. In all experiments, male and female mice aged 8–30 weeks between 25 and 35 g body weight were used.

Drugs and routes of administration

All drugs were freshly prepared prior to use and were injected subcutaneously (s.c.) or intraperitoneally (i.p.) in unanaesthetized mice at a volume of 10 µl/g bodyweight. Opioid drugs were diluted in 0.9% (w/v) saline and cannabinoid drugs in vehicle solution, containing 13.2% ethanol and 0.25%Tween80 in 0.9% saline, for injections. Drugs were obtained and used as follows: fentanyl citrate (0.3 mg/kg for 15 min; s.c.) (B. Braun 06900650), levomethadone hydrochloride (15 mg/kg for 30 min; s.c.) (Sanofi-Aventis 07480196), naloxone (2 mg/kg for 25 min; s.c.) (Ratiopharm 04788930), CP-55940 (0.75 mg/kg for 30 min; i.p.) (Sigma-Aldrich C1112) and AM251 (3 mg/kg for 45 min; i.p.) (MedChemExpress

183232-66-8). CP-55940 was dissolved in vehicle solution containing ethanol, NaCl and Tween80. A total of 35 mice (n=4-6 per treatment condition) were used.

Immunohistochemistry

Mice were deeply anaesthetized with isoflurane (CP-Pharma 4001404) and then subjected to a transcardial perfusion with calcium-free Tyrode's solution containing protein phosphatase-inhibitors (+PPIs) (1 tablet PhosSTOP per 10 ml) (Roche 04906845001) followed by Zamboni's fixative containing 4% paraformaldehyde and 0.2% picric acid in 0.1 M phosphate buffer pH 7.4 +PPIs. Brains and spinal cords were rapidly dissected and postfixed in the same fixative for 4 h at room temperature. The tissue was cryoprotected by immersion in 10% sucrose +PPIs followed by 30% sucrose +PPIs for 48 h at 4 °C before sectioning using a freezing microtome. Tissue was cut into 40 µm sections. Free-floating sections were washed in PBS +PPIs and incubated in methanol containing 0.3% H_2O_2 for 30 min. After washing in PBS-T (PBS + 0,3% Tween®20), the sections were blocked in PBS containing 0.3% Triton X-100, PPIs and 10% NGS for 2 h. Subsequently, the sections were incubated with primary antibody in PBS containing 0.3% Triton X-100, 2% NGS +PPI overnight at 4°C. Where indicated, primary antibodies were preincubated with 1 µg/ml of their cognate phospho-peptide or the corresponding non-phospho-peptide for 1 h at room temperature. Staining of primary antibody was detected using the biotin amplification procedure as described [29, 30]. Briefly, tissue sections were transferred to biotinylated donkey anti-rabbit IgG (1:300 in PBS containing 0.3% Triton X-100, PPIs and 10% NGS) for 2 h, washed in PBS-T plus PPIs and then incubated in AB solution (reagents from the Vector ABC kit; 25 µl A and 25 µl B in 10 ml PBS+0.3% Triton X-100 and PPIs) for 60 min, washed again in PBS-T plus PPIs and transferred to biotinylated tyramine (BT) solution (BT was prepared as described by Adams [31], 5 µl BT+0.01% H_2O_2 in 1 ml PBS+0.3% Triton X-100 and PPIs) for 20 min, followed by a

final incubation step in streptavidin-AlexaFluor555 conjugate 1:400 in PBS+0.3% Triton X-100 containing 10% NDS + PPI) overnight at 4°C. Sections were then mounted onto SuperFrost Plus glass slides (ThermoFisher 15438060) and cover slipped with Eukitt (ORSAtec). Specimens were examined using a Zeiss LSM 900 laser scanning confocal microscope equipped with ZEN software for image analysis.

Data availability

All data supporting the findings of this study are available within the article and its supplementary information files. Additional information, relevant data and unique biological materials will be available from the corresponding author upon reasonable request. Source data are provided with this paper.

References

1. Drube, J. et al. GPCR kinase knockout cells reveal the impact of individual GRKs on arrestin binding and GPCR regulation. *Nat Commun* **13**, 540 (2022).
2. Gurevich, E.V., Tesmer, J.J., Mushegian, A. & Gurevich, V.V. G protein-coupled receptor kinases: more than just kinases and not only for GPCRs. *Pharmacol Ther* **133**, 40-69 (2012).
3. Liggett, S.B. Phosphorylation barcoding as a mechanism of directing GPCR signaling. *Sci Signal* **4**, pe36 (2011).
4. Premont, R.T. & Gainetdinov, R.R. Physiological roles of G protein-coupled receptor kinases and arrestins. *Annu Rev Physiol* **69**, 511-534 (2007).
5. Tobin, A.B., Butcher, A.J. & Kong, K.C. Location, location, location...site-specific GPCR phosphorylation offers a mechanism for cell-type-specific signalling. *Trends Pharmacol Sci* **29**, 413-420 (2008).
6. Doll, C. et al. Agonist-selective patterns of micro-opioid receptor phosphorylation revealed by phosphosite-specific antibodies. *Br J Pharmacol* **164**, 298-307 (2011).
7. Grecksch, G. et al. Analgesic tolerance to high-efficacy agonists but not to morphine is diminished in phosphorylation-deficient S375A mu-opioid receptor knock-in mice. *J Neurosci* **31**, 13890-13896 (2011).
8. Just, S. et al. Differentiation of opioid drug effects by hierarchical multi-site phosphorylation. *Mol Pharmacol* **83**, 633-639 (2013).
9. Prihandoko, R., Bradley, S.J., Tobin, A.B. & Butcher, A.J. Determination of GPCR Phosphorylation Status: Establishing a Phosphorylation Barcode. *Curr Protoc Pharmacol* **69**, 2 13 11-12 13 26 (2015).
10. Divorty, N. et al. Agonist-induced phosphorylation of orthologues of the orphan receptor GPR35 functions as an activation sensor. *J Biol Chem*, 101655 (2022).

11. Illing, S., Mann, A. & Schulz, S. Heterologous regulation of agonist-independent mu-opioid receptor phosphorylation by protein kinase C. *Br J Pharmacol* **171**, 1330-1340 (2014).

12. Mann, A. et al. New phosphosite-specific antibodies to unravel the role of GRK phosphorylation in dopamine D2 receptor regulation and signaling. *Sci Rep* **11**, 8288 (2021).

13. Mann, A. et al. Agonist-induced phosphorylation bar code and differential post-activation signaling of the delta opioid receptor revealed by phosphosite-specific antibodies. *Sci Rep* **10**, 8585 (2020).

14. Mann, A. et al. Agonist-selective NOP receptor phosphorylation correlates in vitro and in vivo and reveals differential post-activation signaling by chemically diverse agonists. *Sci Signal* **12** (2019).

15. Miess, E. et al. Multisite phosphorylation is required for sustained interaction with GRKs and arrestins during rapid mu-opioid receptor desensitization. *Sci Signal* **11** (2018).

16. Kliewer, A., Reinscheid, R.K. & Schulz, S. Emerging Paradigms of G Protein-Coupled Receptor Dephosphorylation. *Trends Pharmacol Sci* **38**, 621-636 (2017).

17. Doll, C. et al. Deciphering micro-opioid receptor phosphorylation and dephosphorylation in HEK293 cells. *Br J Pharmacol* **167**, 1259-1270 (2012).

18. Lehmann, A., Kliewer, A., Gunther, T., Nagel, F. & Schulz, S. Identification of Phosphorylation Sites Regulating sst3 Somatostatin Receptor Trafficking. *Mol Endocrinol* **30**, 645-659 (2016).

19. Lehmann, A., Kliewer, A., Martens, J.C., Nagel, F. & Schulz, S. Carboxyl-terminal receptor domains control the differential dephosphorylation of somatostatin receptors by protein phosphatase 1 isoforms. *PLoS One* **9**, e91526 (2014).

20. Petrich, A. et al. Phosphorylation of threonine 333 regulates trafficking of the human sst5 somatostatin receptor. *Mol Endocrinol* **27**, 671-682 (2013).

21. Poll, F., Doll, C. & Schulz, S. Rapid dephosphorylation of G protein-coupled receptors by protein phosphatase 1beta is required for termination of beta-arrestin-dependent signaling. *J Biol Chem* **286**, 32931-32936 (2011).

22. Tran, T.M. et al. Characterization of beta2-adrenergic receptor dephosphorylation: Comparison with the rate of resensitization. *Mol Pharmacol* **71**, 47-60 (2007).

23. Waser, B. et al. Phosphorylation of sst2 receptors in neuroendocrine tumors after octreotide treatment of patients. *Am J Pathol* **180**, 1942-1949 (2012).

24. Fritzwanker, S. et al. HA-MOP knockin mice express the canonical micro-opioid receptor but lack detectable splice variants. *Commun Biol* **4**, 1070 (2021).

25. Kliewer, A. et al. Phosphorylation-deficient G-protein-biased mu-opioid receptors improve analgesia and diminish tolerance but worsen opioid side effects. *Nat Commun* **10**, 367 (2019).

26. Davis, M.I. et al. The cannabinoid-1 receptor is abundantly expressed in striatal striosomes and striosome-dendron bouquets of the substantia nigra. *PLoS One* **13**, e0191436 (2018).

27. Santos, R. et al. A comprehensive map of molecular drug targets. *Nat Rev Drug Discov* **16**, 19-34 (2017).

28. Percie du Sert, N. et al. The ARRIVE guidelines 2.0: Updated guidelines for reporting animal research. *PLoS Biol* **18**, e3000410 (2020).

29. Schreff, M. et al. Distribution, targeting, and internalization of the sst4 somatostatin receptor in rat brain. *J Neurosci* **20**, 3785-3797 (2000).

30. Schulz, S. et al. Immunolocalization of two mu-opioid receptor isoforms (MOR1 and MOR1B) in the rat central nervous system. *Neuroscience* **82**, 613-622 (1998).

31. Adams, J.C. Biotin amplification of biotin and horseradish peroxidase signals in histochemical stains. *J Histochem Cytochem* **40**, 1457-1463 (1992).

Acknowledgements: We want to thank Svetlana Würl and Monique Brendel for expert technical assistance. This work was supported by the European Regional Development Fund (EFRE) and the Free State of Thuringia (grant: 2020 FE 0146) to 7TM Antibodies GmbH.

Author contributions: S.S. conceived and initiated the project and designed all experiments with S.F. . S.F. and A.K. performed and analyzed immunohistochemistry. F.N. affinity-purified all phosphosite-specific antibodies used in this study. The manuscript was written and revised by S.S. and S.F. with input from other authors.

Competing interests: S.S. is the founder and scientific advisor of 7TM Antibodies GmbH, Jena, Germany. F.N. is an employee of 7TM Antibodies. All other authors declare no competing interests.

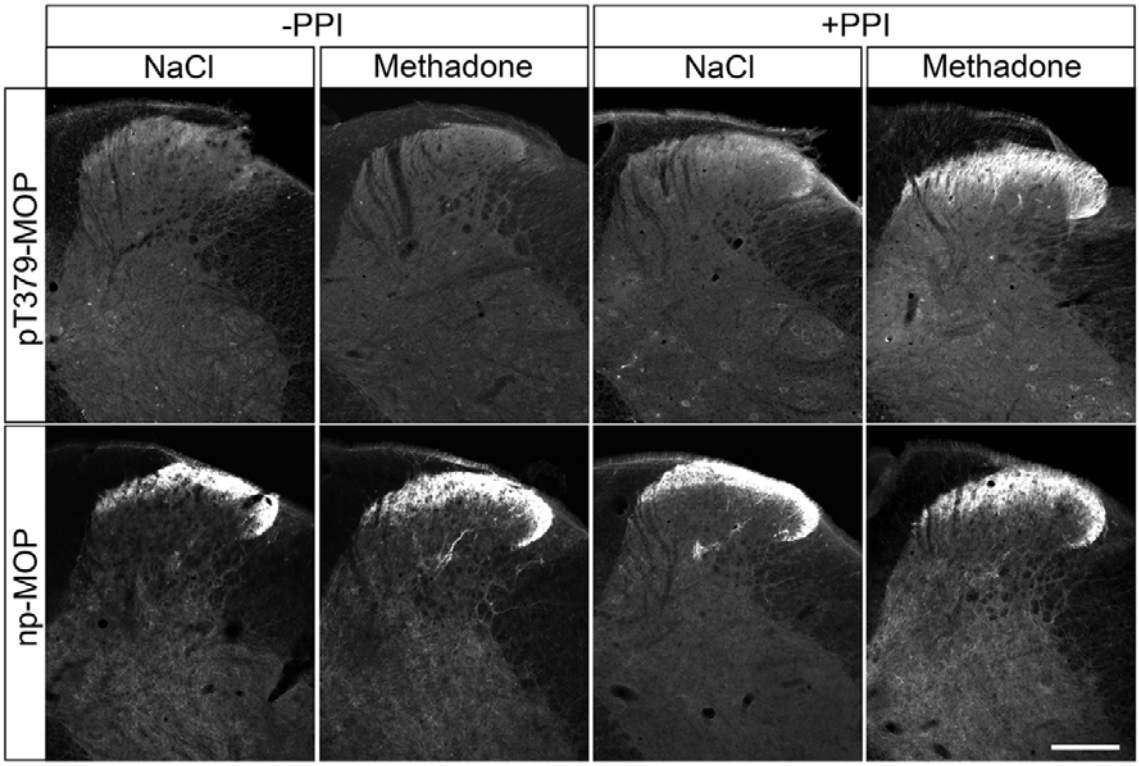

Fig. 1. Comparison of phospho-MOP immunohistochemistry in the presence or absence of protein phosphatase inhibitors. (A, B) Animals were either treated with methadone or saline for 30 min, transcardially perfused, fixed and stained in the presence (+) or absence (-) of protein phosphatase inhibitors (PPI). Shown are confocal images of coronal sections of the spinal cord stained with pT379-MOP or np-MOP antibody. Note that PPIs need to be present during both fixation and staining procedures to obtain agonist-induced phospho-MOP immunostaining. Scale bar = 250 µm.

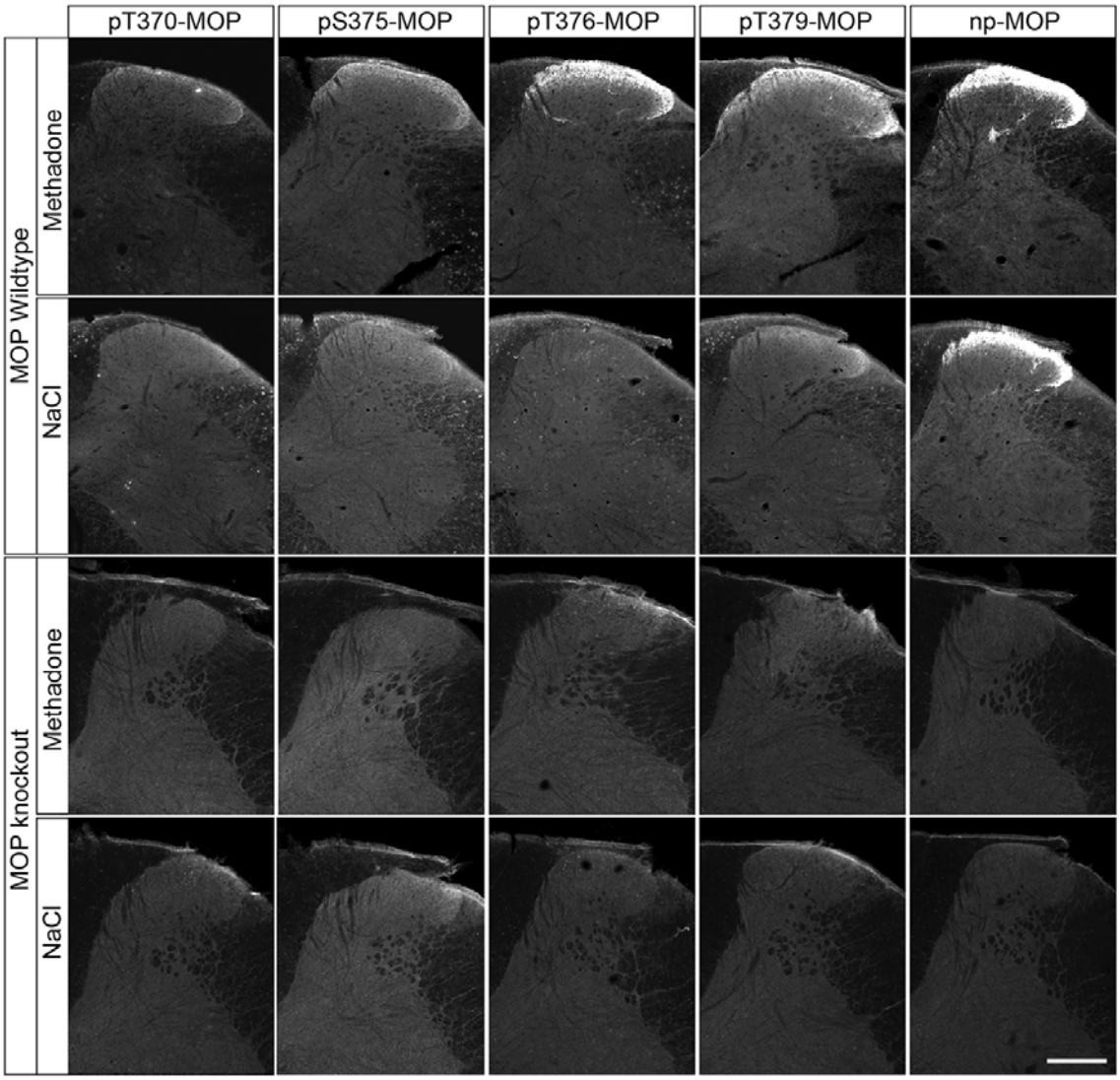

Fig. 2. Immunohistochemical staining of agonist-induced MOP phosphorylation in the mouse spinal cord. Animals were treated with methadone or saline for 30 min, transcardially perfused, fixed and stained in the presence of PPIs. Shown are confocal images of coronal sections of the spinal cord stained with phosphosite-specific antibodies pT370-MOP, pS375-MOP, pT376-MOP and pT379-MOP, or phosphorylation independent np-MOP antibody. Note that pS375-MOP, pT376-MOP and pT379-MOP, but not pT370-MOP, revealed an agonist-dependent MOP phosphorylation immunostaining in a pattern closely resembling that of agonist-independent np-MOP imunostaining. Scale bar = 250 µm.

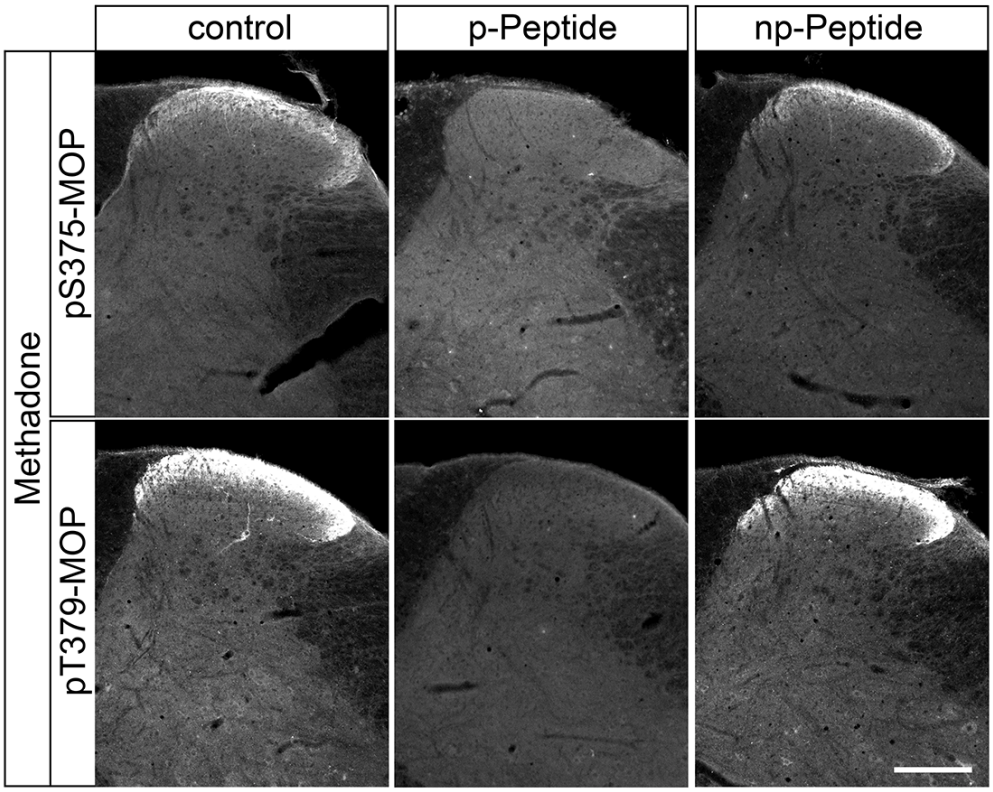

Fig. 3. Peptide neutralization of agonist-induced MOP phosphorylation staining in the mouse spinal cord. Animals were treated with methadone for 30 min, transcardially perfused, fixed and stained in the presence of PPIs. Shown are confocal images of coronal sections of the spinal cord stained with phosphosite-specific antibodies pS375-MOP or pT379-MOP in the presence or absence of their immunizing peptides containing S375 or T379 in phosphorylated form (p-Peptide) or the corresponding non-phosphorylated peptide (np-Peptide). Note that phospho-MOP immunostaining was completely neutralized by excess of phosphorylated peptide but not of non-phosphorylated peptide. Scale bar = 250 µm.

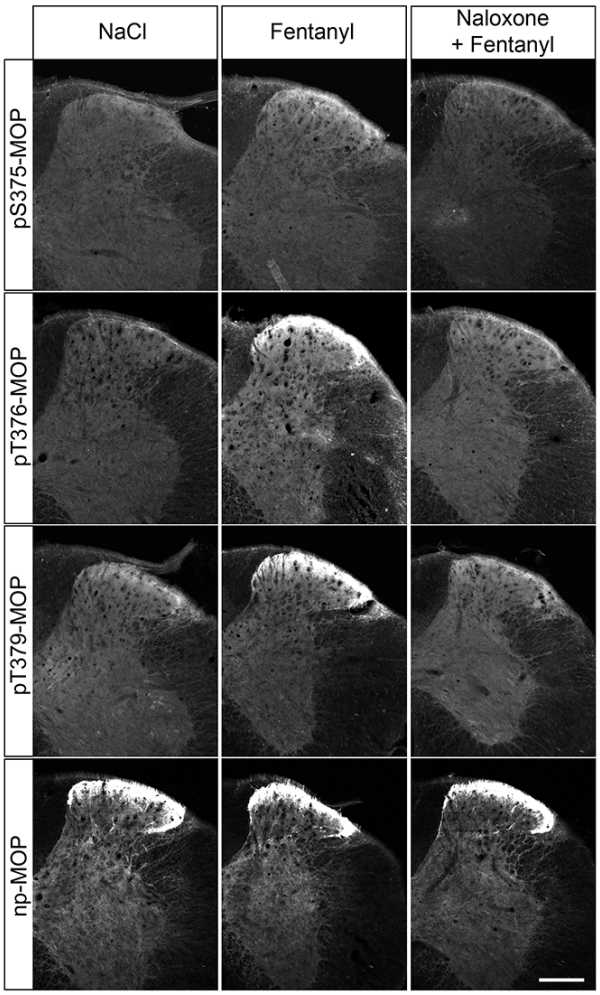

Fig. 4. Antagonist block of phospho-MOP immunostaining. Animals were either treated with saline or fentanyl for 15 min. Where indicated, animals were pretreated with naloxone for 10 min followed by 15-min fentanyl treatment. Animals were then transcardially perfused, fixed and stained in the presence of PPIs. Shown are confocal images of coronal sections of the spinal cord stained with phosphosite-specific antibodies pS375-MOP, pT376-MOP or pT379-MOP or phosphorylation independent np-MOP antibody. Note that agonist-induced phopho-MOP immunostaining is diminished by antagonist treatment. Scale bar = 250 µm.

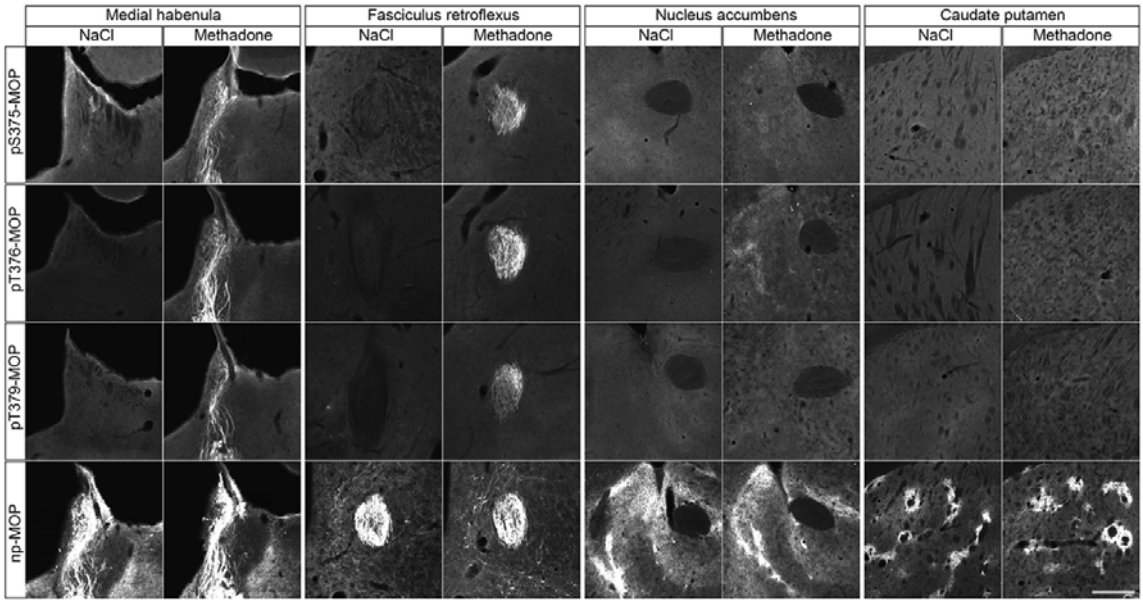

Fig. 5. Agonist-induced phospho-MOP immunostaining in mouse brain. Animals were treated with methadone for 30 min, transcardially perfused, fixed and stained in the presence of PPIs. Shown are confocal images of coronal brain sections stained with phosphosite-specific antibodies pS375-MOP, pT376-MOP or pT379-MOP or phosphorylation independent np-MOP antibody. Note that all three phosphosite-specific antibodies detected agonist-induced MOP phosphorylation in the medial habenula and fasciculus retroflexus but not in caudate putamen, a brain region known to be rich in MOP receptors as shown by np-MOP antibody staining. Scale bar = 250 µm.

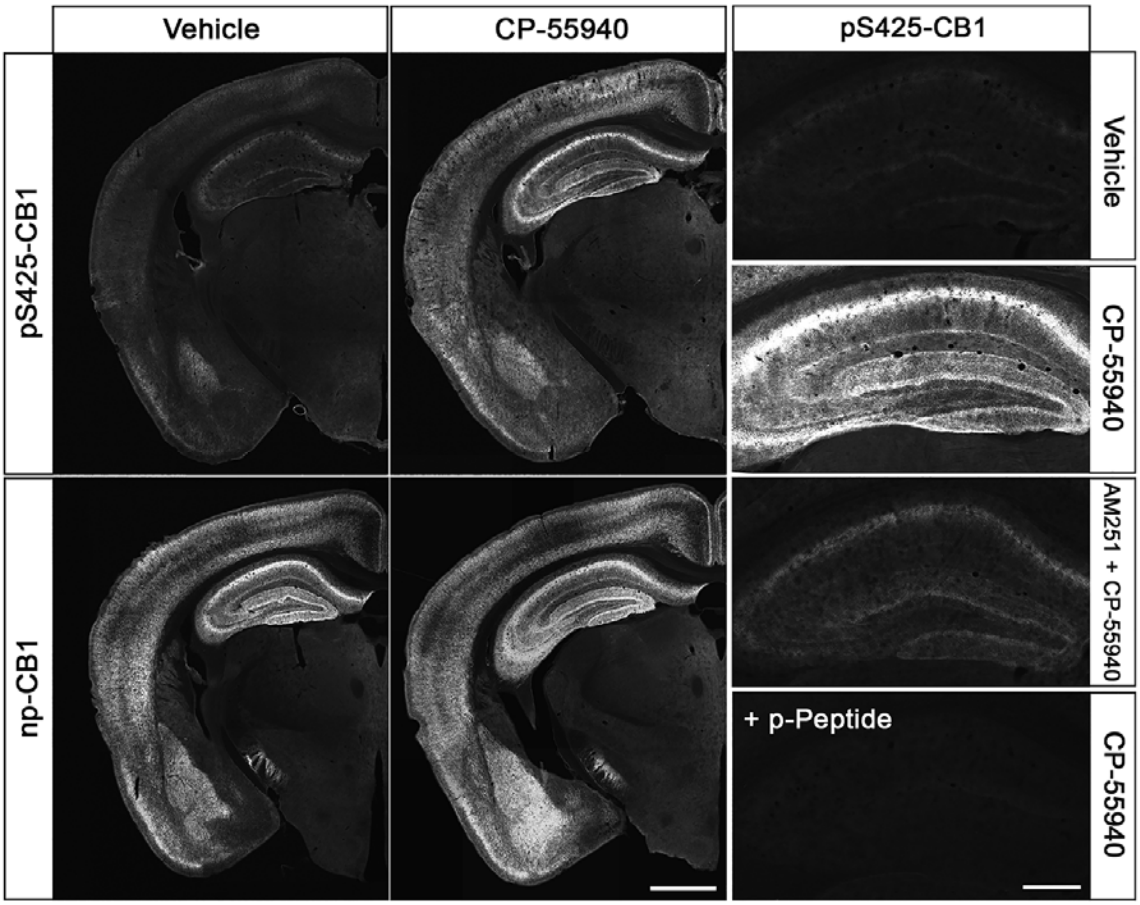

Fig. 6. Agonist-induced phospho-CB1 immunostaining in mouse brain. Animals were either treated with Vehicle or CP-55940 for 30 min. Where indicated, animals were pretreated with AM251 for 45 min followed by 30-min CP-55940 treatment. Animals were then transcardially perfused, fixed and stained in the presence of PPIs. Shown are confocal images of coronal brain sections stained with phosphosite-specific antibody pS425-CB1, in the presence or absence of the p-Peptide containing S425 in phosphorylated form, or phosphorylation independent np-CB1 antibody. Note that agonist-induced phopho-CB1 immunostaining is diminished by antagonist treatment. Note that phospho-CB1 immunostaining was completely neutralized by excess of phosphorylated peptide. Scale bar = 1000 µm and 250 µm.

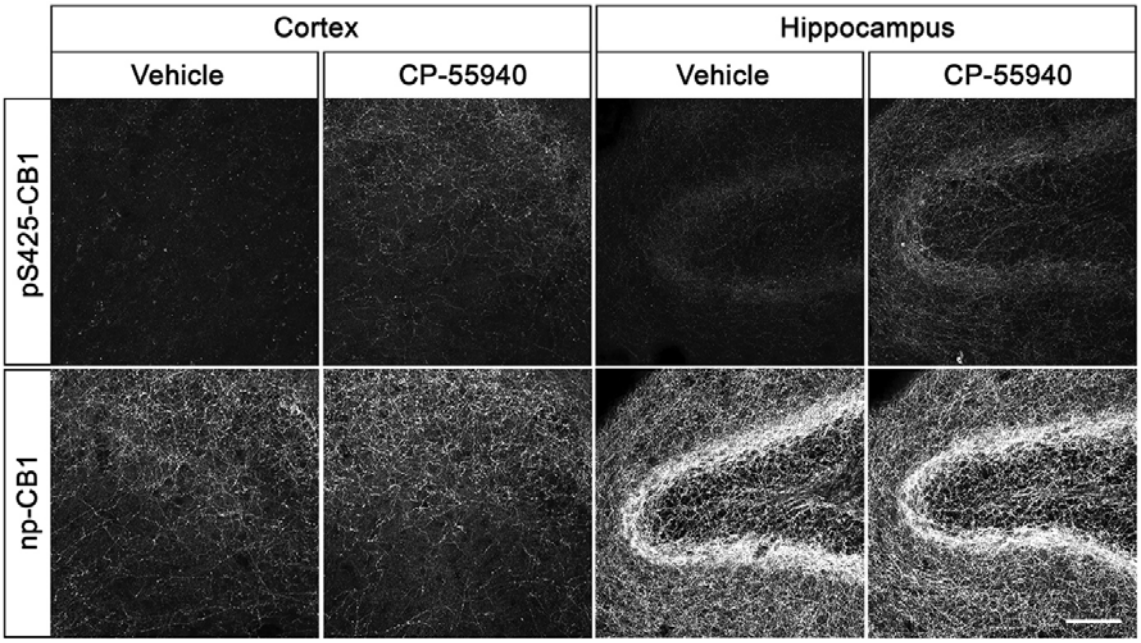

Fig. 7. Agonist-induced phospho-CB1 immunostaining in mouse brain. Animals were either treated with Vehicle or CP-55940 for 30 min. Animals were then transcardially perfused, fixed and stained in the presence of PPIs. Shown are confocal images of coronal brain sections stained with phosphosite-specific antibody pS425-CB1. Note that agonist-induced phopho-CB1 immunostaining is localized to fibers and terminals in cortex and hippocampus. Scale bar = 100 µm.